

# A one-step microfluidic approach for controllable preparation of nanoparticle-coated patchy microparticles

Wenjie Lan · Shaowei Li · Jianhong Xu ·  
Guangsheng Luo

Received: 27 February 2012 / Accepted: 8 April 2012 / Published online: 24 April 2012  
© Springer-Verlag 2012

**Abstract** In this work, we describe a one-step microfluidic method for fabricating nanoparticle-coated patchy particles. Janus droplets composed of curable phase and non-curable phase were produced via a co-axial microfluidic device first. Nanoparticles were dispersed into the continuous phase or the non-curable phase to realize the surface coating of the curable phase. The curable phase was then polymerized by UV light and nanoparticle-coated patchy particles were obtained. The SEM characterization shows that the particles are monodispersed with nanoparticle selectively distributed on the convex or concave surface. The dispersity, size and shape of the particles could be easily controlled by changing the microfluidic flow parameters. Three different types of nanoparticles were successfully used to synthesize the patchy particles to demonstrate the validity of the method.

**Keywords** Patchy microparticles · Microfluidic device · Nanoparticles · Surface coating

## 1 Introduction

Anisotropic particles have recently attracted much attention. The lack of centro symmetry in synthetic anisotropic systems has led to the discovery of novel material properties that are impossible to attain with homogeneous or

symmetric materials (Du and O'Reilly 2011; Walther and Muller 2008). Anisotropic particles have been used as building blocks (Gracias et al. 2000; Lu et al. 2001; Perro et al. 2005; Jiang et al. 2008; Binks and Fletcher 2001), emulsion stabilizers (Dinsmore et al. 2002; Blinks and Clint 2002), micro-rheological probes (Behrend et al. 2004), light diffusers (Takei and Shimizu 1997; Graham-Rowe 2007), etc. Particle anisotropy may arise from their non-spherical shape or their non-uniform intrinsic properties. Particles with non-uniform surface properties could be divided into two classes: particles composed of multi-compartment (multi-compartment particles) and particles with patches of varying surface (patchy particles).

Fabrication of patchy particles is usually based on site-selective modification of the surfaces of spherical particles to obtain particles with intrinsic asymmetry. The most common preparation techniques include microcontact printing, gel trapping, masking/unmasking techniques and Pickering emulsion method (Cayre et al. 2003; Paunov and Cayre 2004; Bao et al. 2002; Ling et al. 2009; Hong et al. 2006). In all of these methods, the following stages are necessarily included: the preparation of monodispersed particles, the arrangement of the target particles at a gas-liquid, liquid-liquid or liquid-solid interface and the attachment of the desired agents from one phase. The multi-step procedure is time-consuming and frequent batch-to-batch process would adversely influence the reproducibility. Therefore, it would be intriguing if patchy particles could be synthesized in a single step.

Our research aims to present an alternative to the commonly used preparation method for patchy particles by use of biphasic droplets formed by liquid/liquid/liquid three-phase microflow. In this method, uniform biphasic Janus droplets composed of curable and non-curable phase are generated first, and then the curable phase is solidified

W. Lan · S. Li · J. Xu (✉) · G. Luo (✉)  
The State Key Lab of Chemical Engineering,  
Department of Chemical Engineering,  
Tsinghua University, Beijing 100084, China  
e-mail: xujianhong@tsinghua.edu.cn

G. Luo  
e-mail: gsluo@tsinghua.edu.cn

to form non-spherical particles. Meanwhile, the nanoparticles for surface modification could contact the curable phase from either the continuous phase or the non-curable phase to realize asymmetrical modification.

This method requires the generation of biphasic Janus droplet with uniform size and composition, which is extremely difficult to achieve by traditional emulsion method. Microfluidic devices have recently emerged as a powerful tool for the precise control of emulsion structure. Significant advances have been made in the use of microfluidic devices for controlling multiphase flow patterns and numerous studies on stable microfluidic flow patterns such as homogeneous drops and slugs flow (Thorsen et al. 2001; Nisisako et al. 2002; Xu et al. 2006a), drop-in-drop flow (Garstecki et al. 2006; Wang et al. 2011; Abate et al. 2010; Saeki et al. 2010) and co-laminar flow (Lan et al. 2010). Steady and uniform biphasic drop flow has also been formed in microfluidic devices and used to fabricate monodispersed Janus particles (Chen et al. 2009; Prasad et al. 2009; Nisisako and Torii 2007; Nisisako and Hattuzawa 2010; Nie et al. 2005). Therefore, the microfluidic technology may provide a promising route for one-step patchy particle fabrication (Kim et al. 2011).

In our previous work, homogeneous nanoparticle-coated particles have been fabricated via microfluidic technology (Lan et al. 2011). The results indicate that the process of in situ surface coating with nanoparticles in microdevices is controllable and highly effective. In this study, a novel and simple method for the in situ synthesis of patchy particles was developed using Janus drop flow in a coaxial microfluidic device. Non-spherical microparticles with unsymmetrical surface coating by nanoparticles were prepared in a single step. The monodispersity, size and shape of the microparticles were characterized, and the influences of different operation conditions were discussed. Three types of nanoparticles were selected as the coating materials and selectively coated onto different sites of the non-spherical particles.

## 2 Experiments

### 2.1 Materials

For the generation of biphasic droplets, 1,6-hexanediol diacrylate (HDDA, Sigma-Aldrich, USA) and low viscosity silicone oil (10cst, Sigma-Aldrich, USA) were used as the photocurable phase and the non-curable phase, respectively. Photoinitiator 2-hydroxy-2-methylpropiophenone (Sigma-Aldrich, USA) and oil-soluble dye Oil Blue N (Sigma-Aldrich, USA) were dissolved in the curable phase. A sodium dodecyl sulfate (SDS, VAS Chemical Co., Ltd., Tianjin, P.R. China) aqueous solution was used

as the continuous phase. In each experiment, Titanium silicate molecular sieve nanoparticles (TS-1, Midwest Chemical Co., Ltd., P.R. China) or polystyrene beads (fluorescent red, Sigma-Aldrich, USA) with diameters of approximately 300 and 500 nm, respectively, were dispersed in the continuous phase as the coating material for surface A. Hydrophobic SiO<sub>2</sub> nanoparticles (Nachen S&T Ltd., Beijing, P.R. China) with diameter of 30 nm were dispersed in the silicon oil as the coating material for surface B.

### 2.2 Experimental microfluidic device

A flow chart of the experiment and the microfluidic device is shown in Fig. 1a. The device was fabricated on a 60 × 20 × 3 mm PMMA chip using micromachining technology. A glass tube (I.D. 600 μm) was inserted as the main channel for the multiphase flow, while another glass tube with a shrink tip was inserted into the main channel as the dispersed phase channel. The inner diameter of the dispersed phase glass tubes and the shrink tip was 700 and 50 μm, respectively. Two stainless steel microneedles were inserted into the dispersed phase channel as the inlet of curable phase and silicone oil. The outer and inner diameter of the microneedle was 330 μm and 160 μm, respectively. The microfluidic device was sealed using another 60 × 20 × 1 mm PMMA chip which was bonded to the first chip using the ultrasonic-assisted sealing technique (Li et al. 2009). Three microsyringe pumps and four gastight microsyringes were used to pump the fluids into the microfluidic device. The outlet of the glass tube was exposed to a UV light to control the polymerization of the curable phase.

### 2.3 Preparation of nanoparticle-coated patchy particles

In each experiment, a solution with 1 % wt photoinitiator and 99 % wt HDDA was used as the curable phase. Silicone oil was used as the non-curable phase. Oil-soluble dyes were dissolved in the curable phase to distinguish the two phases. The two phases were pumped into the microdevice through two microneedles. A stable co-laminar flow formed in the dispersed phase channel. An aqueous solution with 2 % wt SDS was used as the continuous phase. As the dispersed phase flowed through the shrink tip, monodispersed Janus droplets were produced by the sheath focusing force of the continuous phase flow.

For the fabrication of surface A coated patchy particles, TS-1 nanoparticles or polystyrene beads were added to the continuous phase at concentration of 1 % wt. For the preparation of surface B coated patchy particles, SiO<sub>2</sub> nanoparticles were added to silicone oil at concentration of 0.5 %wt. Nanoparticles were uniformly dispersed in the

**Fig. 1** **a** Flow chart of the experiments. **b** Flow patterns observed from the frame in **a** with different non-curable phase flow rate ( $Q_s$ ) and curable phase flow rate ( $Q_h$ ). The dyed curable phase is pumped through the upper microneedle and the non-curable phase is pumped through the lower microneedle. **c** Micrographs of the Janus droplets in a glass culture plate; 1 just out flowed from the channel, 2 kept in the container for more than 1 min. **d** Effects of continuous phase flow rate  $Q_c$  on the droplet diameter  $d$ . ( $Q_s$  40  $\mu\text{L}/\text{min}$ ,  $Q_h$  10 $\mu\text{L}/\text{min}$ ). **e** SEM images of the asymmetrical particles at different dispersed phase flow ratios: 1  $Q_h/Q_s$  1/4, 5  $Q_h/Q_s$  2/1 and 6  $Q_h/Q_s$  1/0. 2, 3 SEM images of the different surface of the asymmetrical particle 2 surface A and 3 surface B. 4 EDS spectrum of the asymmetrical particle at surface area 1 in **e**, 2

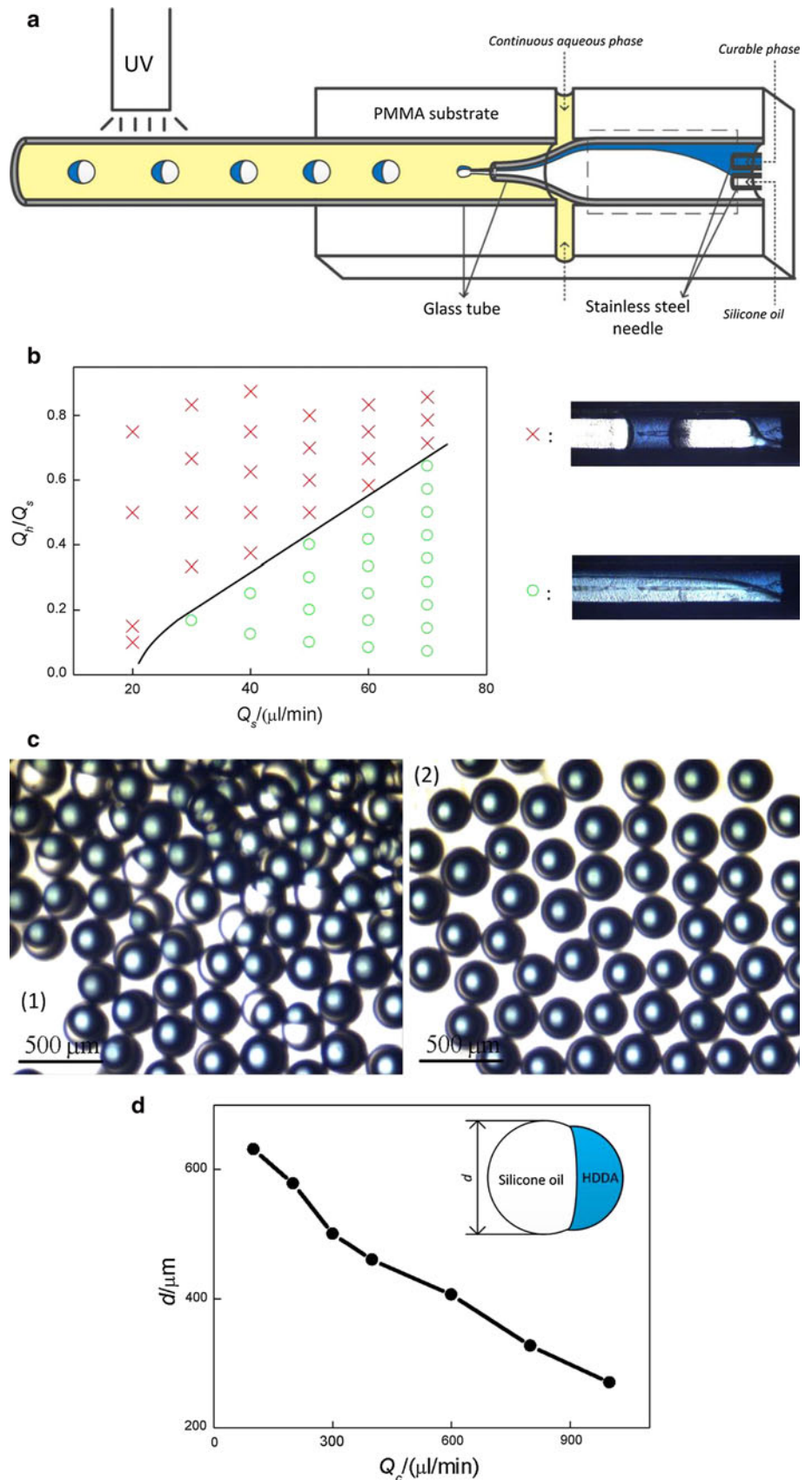
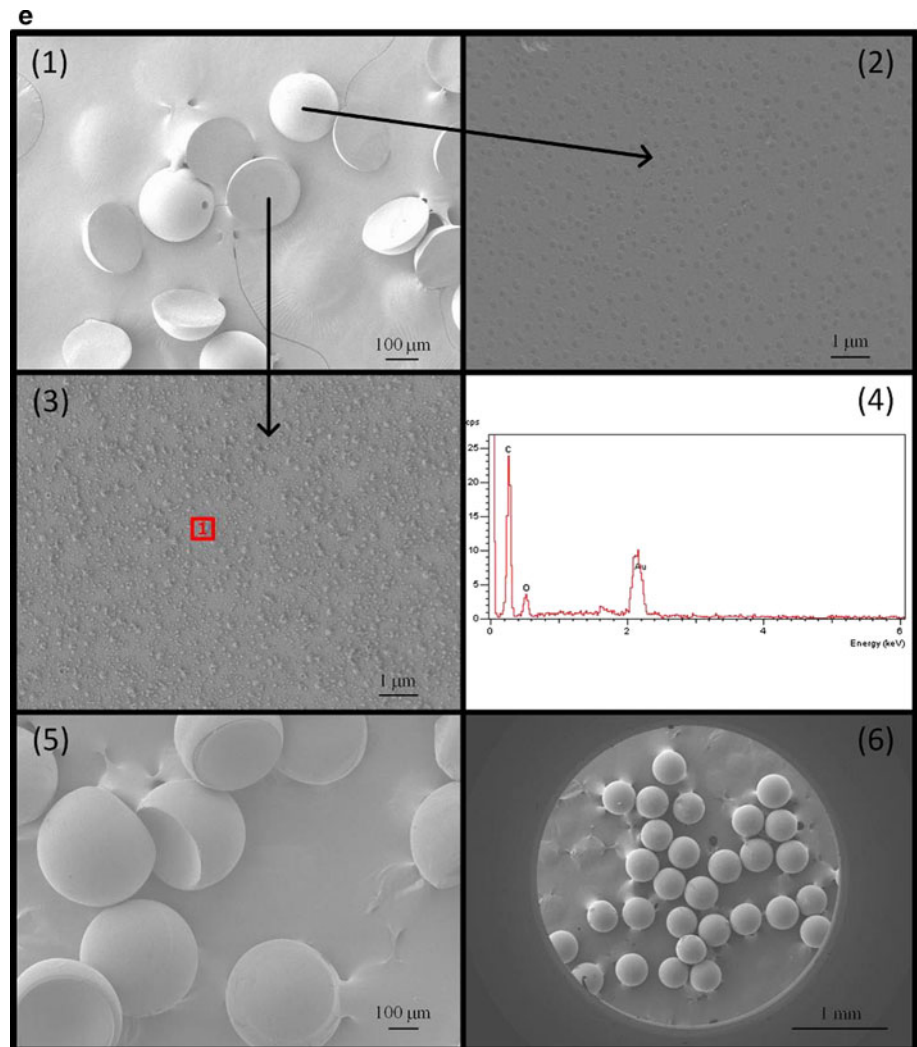


Fig. 1 continued



continuous phase by sonicating for more than 60 min. The nanoparticle concentration should not be too high to make them easily agglomerate and deposit from the fluids. At the end of the main channel, the particles were photopolymerized by exposing to the UV light. The obtained particles were washed with ethanol and collected.

#### 2.4 Characterization

Droplet formation and the microflows were observed with an optical microscope coupled with a high-speed CCD video camera (Olympus). More detailed structures were observed using scanning electron microscopy (SEM, FEI XL30) operating at 1 kV. Energy spectrum analysis (EDS) was performed on the SEM samples using the EDS function of the SEM. Rhodamine B was used as a fluorescent marker in our experiments. Fluorescence was observed by using a confocal laser scanning microscopy (DSU, Olympus).

### 3 Results and discussion

#### 3.1 Janus droplet and asymmetrical microparticle formation

The microfluidic device is composed of a uniform glass tube as the main channel and a glass tube with a shrink tip as the dispersed phase channel. Curable and non-curable dispersed phase were introduced into the dispersed phase channel. To obtain monodispersed Janus droplet, the two organic dispersed phases should form the stable liquid/liquid co-laminar flow regime before flowing out from the shrink tip. Therefore, the determination of the two-phase flow is very important. We investigated the flow patterns in the dispersed phase glass tube as shown in Fig. 1b. The stable co-laminar flow could be easily formed when the flow conditions are well selected. A transition line in Fig. 1b can be used to identify the co-laminar flow from



other flows, including unstable co-laminar flow, slug flow and droplet flow.

At the outlet of the shrink tip, the dispersed phase is sheared by the continuous aqueous phase to form monodispersed Janus droplets. Figure 1c shows the micrographs of formed droplets. The droplets are highly uniform and could exist stably without coalescence or breakup of the two components. Previous studies have shown that the droplet formation is determined by the balance between the shear and interfacial forces (Utada et al. 2007; Cramer et al. 2004; Cristini and Tan 2004; Xu et al. 2006b). For the experimental systems used, there was very little variation in the liquid phase viscosities and liquid–liquid interfacial tension. Besides, the influence of the dispersed phase flow rate on droplet size is slight (Burns and Ramshaw 2001; Gunther et al. 2005; Waelchli and von Rohr 2006; Tung et al. 2009). Thus, the droplet size is mainly influenced by the continuous flow rate. The detailed investigation of the influence of flow rate on droplet size was carried out and the results are shown in Fig. 1d. The droplet size decreases with the increase of the continuous phase flow rate. Therefore, we can easily control the droplet size by changing the continuous phase flow rate (supported by Figure S1). The droplet average diameter ranged from 200 to 600  $\mu\text{m}$  in our work.

Furthermore, by adjusting the ratio of the curable and non-curable phase flow rates, we could control the ratio of the curable phase in the droplet and thus the shape of the obtained patchy particles, as shown in Fig. 1e. By adjusting the ratio of the flow fluxes of the two dispersed phases, we could produce the asymmetrical particles with various shapes, as shown in Fig. 1e, 1, 5, 6. The asymmetrical particles are highly uniform in size and shape under the same operation conditions. The surface morphologies of the asymmetrical particles are shown in Fig. 1e, 2, 3. The surface contact with the continuous phase is defined as surface A and the surface contact with the non-curable phase as surface B for convenience. The image shows that no nanoparticles present on surface A. Small granules could be seen on the surface B of the particle. EDS analysis is performed on the granules, as shown in Fig. 1e, 4. Only carbon and oxygen were detected, indicating that the granules are organic compounds.

### 3.2 Nanoparticle-coated patchy particle formation

Then we attempted to in situ prepare nanoparticle-coated anisotropic microparticles by adding the nanoparticles into different phase fluids. Scheme 1 shows the mechanism for generating nanoparticle-coated anisotropic microspheres in our microfluidic approach. It is a recirculation–collision–adsorption process. For the generation of the patchy particles with nanoparticles coated on surface A, nanoparticles are dispersed into the continuous phase. As shown in Scheme 1a, when droplets flow in the channel, there is a recirculation between the droplets because of the friction of the channel wall. There are many reports on the recirculation in the literature (Burns and Ramshaw 2001; Gunther et al. 2005; Waelchli and von Rohr 2006; Tung et al. 2009). This inter-droplet recirculation enhances mixing in the continuous phase and augments the collision between nanoparticles and the droplets. After collision, some of the nanoparticles tend to be adsorbed at the oil–water interface. Nanoparticles adsorbed on the surface are then fixed in place because of curable phase polymerization. After removing the non-curable fluid, the patchy particles with nanoparticles coated only on surface A are obtained. For the generation of the patchy particles with nanoparticles coated on surface B, hydrophobic nanoparticles are dispersed into the non-curable dispersed phase. As shown in Scheme 1b, when droplets flow in the channel, there is also a recirculation in the droplets because of the friction of the continuous phase. Some of nanoparticles tend to be adsorbed at the interface between the two dispersed phases. After polymerization, nanoparticles are fixed on surface B. One of the unique benefits of the microfluidic device is the precise control of each droplet, including the droplet size and the two-phase ratio. Moreover, the microfluidic method generated stable interface in the three-phase system without unwanted droplet breakup and coalescence, which ensures the precise surface modification.

First, we generated patchy particles with nanoparticles coated on surface A. To ensure the uniform dispersion of nanoparticles in the continuous phase, we selected partially hydrophilic titanium silicate (TS-1) nanoparticles as the coating material of surface A. When TS-1 nanoparticles

**Scheme 1** The mechanism of the nanoparticle-coated patchy particles generation process.

**a** Nanoparticles coated on surface A. **b** Nanoparticles coated on surface B

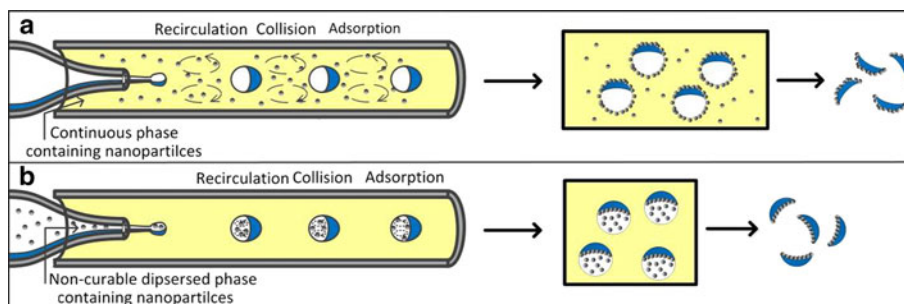


**Fig. 2** **a, b** SEM images of TS-1 nanoparticles coated patchy particle on **a** surface B, **b** surface A. **c** EDS spectrum of the patchy particle at surface area 2 in **a**, **d**) EDS spectrum of the patchy particle at surface area 1 in **b**. Gold is present because the samples are gold coated to prevent charging in the SEM. **e** SEM images of surface A of fluorescent polystyrene beads coated patchy particle. **f** Laser scanning confocal microscopy (LSCM) image of the polystyrene nanoparticles coated patchy microparticles

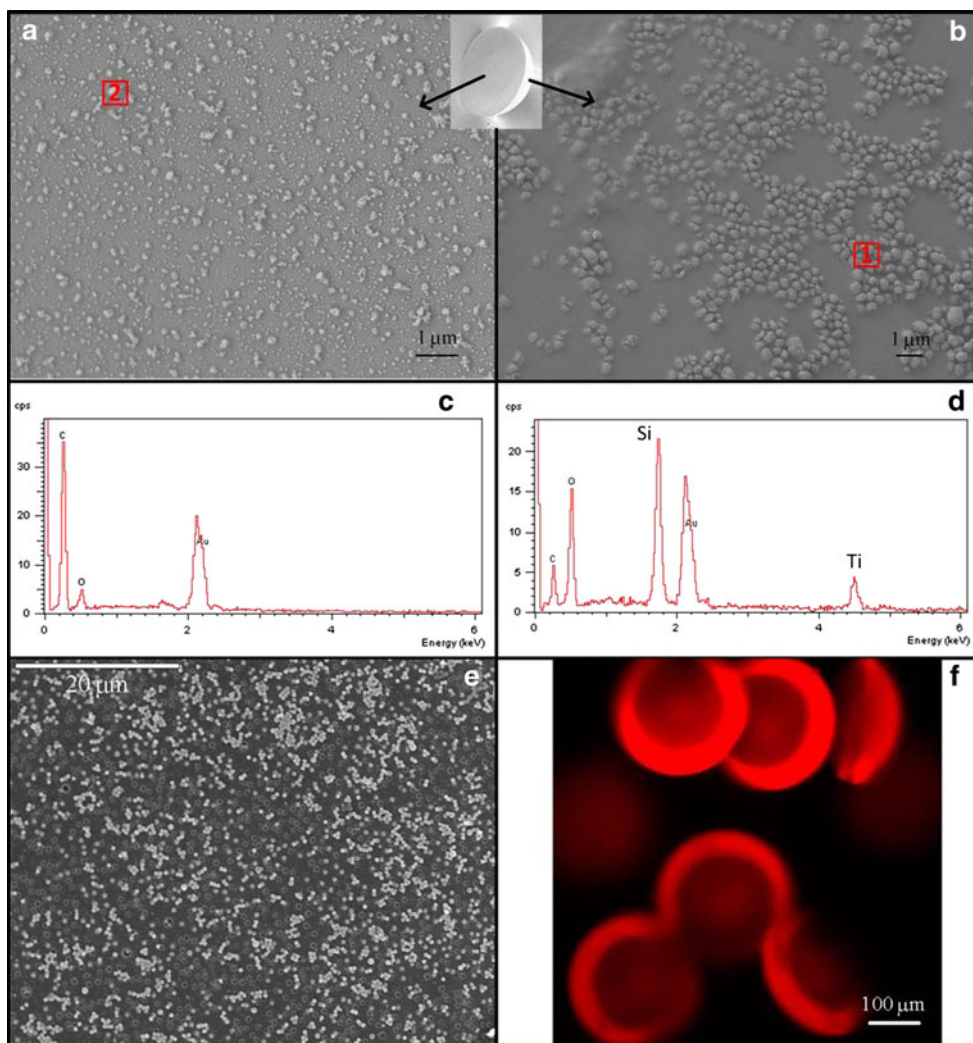
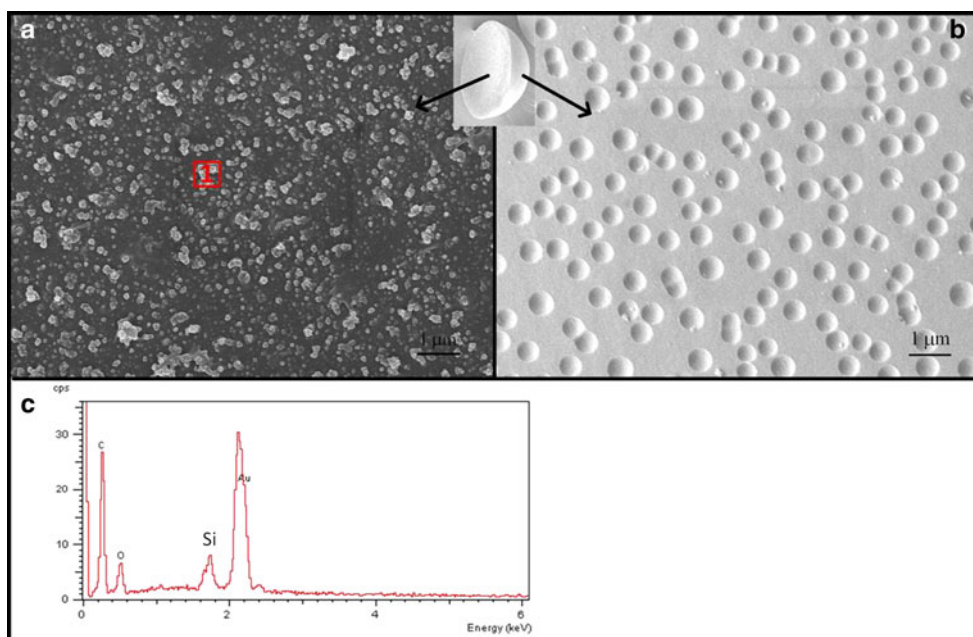


**Fig. 3** **a, b** SEM images of  $\text{SiO}_2$  nanoparticles coated patchy particle on **a** surface B, **b** surface A. **c** EDS spectrum of the patchy particle at surface area 1 in **a**. Gold is present because the samples are gold coated to prevent charging in the SEM



were dispersed into the continuous phase, we obtained patchy microparticles with nanoparticles coated on surface A, as shown in Fig. 2a, b. The images show the uniform distribution of nanoparticles on surface A and the existence of small granules on surface B. EDS analysis was performed on the microparticle surface, as shown in Fig. 2c, d. High levels of silicon and titanium were detected in area 1 of Fig. 2b, while only carbon and oxygen existed in area 2 of Fig. 2a, indicating that TS-1 nanoparticles only coat onto surface A. The above results verify that TS-1 nanoparticle-coated anisotropic microparticles are successfully prepared using the novel microfluidic method in a single step. Furthermore, the patchy microparticles are monodispersed and nanoparticles are uniformly distributed on surface A. Our microfluidic approach to producing hybrid microparticles may be universally applied to many of the partially hydrophilic nanoparticle systems. This is verified in replacing TS-1 nanoparticles by fluorescent carboxylated-modified polystyrene nanoparticles in the continuous phase.

Figure 2e shows that the beads uniformly coat on surface A of the generated patchy microparticles. The morphology of surface B is similar to the TS-1 nanoparticle-coated microparticles shown in Fig. 2a. Besides, only surface A of the patchy microparticles emits fluorescence under irradiation of green laser (Fig. 2f) in the laser scanning confocal microscopy (LSCM) image, which further verifies the asymmetrical surface modification with fluorescent nanoparticles.

On the other hand, for selectively coating of surface B, hydrophobic SiO<sub>2</sub> nanoparticles was selected to ensure the uniform dispersion in silicone oil as well as the adsorption at the oil–oil interface. Figure 3a shows the surface B of the obtained patchy particles, on which nanoparticles are uniformly distributed. The EDS spectrum (Fig. 3c) shows that they are SiO<sub>2</sub> nanoparticles indeed, unlike the pure organic component shown in Fig. 2c. As shown in Fig. 3b, no nanoparticles are present on surface A, which verifies that SiO<sub>2</sub> nanoparticles selectively coat on surface B.

#### 4 Conclusions

In summary, we describe a novel and simple microfluidic approach to prepare nanoparticle-coated patchy microparticles. Monodispersed Janus droplets composed of curable phase and non-curable phase were produced via a co-axial microfluidic device. Nanoparticles were dispersed either in the continuous fluid or the non-curable phase fluid. When the droplets were moving in the channel, nanoparticles were adsorbed onto the interface between the curable phase and the other two phases. The curable phase in the droplets was solidified by UV-irradiated polymerization and the patchy microparticles asymmetrically coated by nanoparticles

were successfully prepared. SiO<sub>2</sub>, TS-1 and fluorescent polystyrene nanoparticles were successfully used as the coating materials, which demonstrated the validity of the method. The microfluidic approach has very good control ability in morphology, monodispersity and size. The morphology of the microparticles could be controlled from less than a hemisphere to a sphere by adjusting the flow rate ratio of the two dispersed phases. The droplet average diameter can be easily controlled from 200 to 600 μm by changing the continuous phase flow rate. The nanoparticle-coated patchy microparticles prepared here would have good potential for being used as heterogeneous reaction catalysts, optical sensors, switchable display devices, etc.

Our method might be universally applied to nanoparticles with specific surface properties. We will do further research to figure out this specific demand. Besides, the loading capacity and stability of nanoparticles on the surface are important hybrid particle properties to consider when determine potential applications. The surface properties, such as wettability and potential, of nanoparticles would significantly influence their dispersion in the original phase, the probability of adsorption at the interface after collision and thus the loading capacity. Meanwhile, surface properties also influence depth of nanoparticles embedded into the curable phase, as well as the combination properties with the polymer surface. All these issues would be further investigated in our future work.

**Acknowledgments** This work was supported by the National Natural Science Foundation of China (21036002, 21136006), National Basic Research Program of China (2012CBA01203), and SRFDP (20090002110070). Supporting Information is available online from Wiley InterScience or from the author.

#### References

- Abate AR, Thiele J, Weinhart M, Weitz DA (2010) Patterning microfluidic device wettability using flow confinement. *Lab Chip* 10:1774–1776
- Bao ZN, Chen L, Weldon M, Chandross E, Cherniavskay O, Dai Y, Tok JBH (2002) Toward controllable self-assembly of microstructures: selective functionalization and fabrication of patterned spheres. *Chem Mater* 14:24–26
- Behrend CJ, Anker JN, McNaughton BH, Roberts TG, Brasuel M, Philert MA, Koperlman R (2004) Metal-capped Brownian and magnetically modulated optical nanoprobes (MOONs): micromechanics in chemical and biological microenvironments. *J Phys Chem B* 108:10408–10414
- Binks BP, Fletcher PDI (2001) Particles adsorbed at the oil-water interface: a theoretical comparison between spheres of uniform wettability and “Janus” particles. *Langmuir* 17:4708–4710
- Blinks BP, Clint JH (2002) Solid wettability from surface energy components: relevance to pickering emulsions. *Langmuir* 18:1270–1273
- Burns JR, Ramshaw C (2001) The intensification of rapid reactions in multiphase systems using slug flow in capillaries. *Lab Chip* 1:10–15

- Cayre O, Paunov VN, Velev ODJ (2003) Fabrication of asymmetrically coated colloid particles by microcontact printing techniques. *Mater Chem* 13:2445–2450
- Chen CH, Shah RK, Abate AR, Weitz DA (2009) Janus particles templated from double emulsion droplets generated using microfluidics. *Langmuir* 25:4320–4323
- Cramer C, Fischer P, Windhab EJ (2004) Drop formation in a co-flowing ambient fluid. *Chem Eng Sci* 59:3045–3058
- Cristini V, Tan YC (2004) Theory and numerical simulation of droplet dynamics in complex flows—a review. *Lab Chip* 4:257–264
- Dinsmore AD, Hsu MF, Nikolaidis MG, Marquez M, Bausch AR, Weitz DA (2002) Colloidosomes: selectively permeable capsules composed of colloidal particles. *Science* 298:1006–1009
- Du JZ, O'Reilly RK (2011) Anisotropic particles with patchy, multicompartment and Janus architectures: preparation and application. *Chem Soc Rev* 40:2402–2416
- Garstecki P, Fuerstman MJ, Stonec HA, Whitesides GM (2006) Formation of droplets and bubbles in a microfluidic T-junction—scaling and mechanism of break-up. *Lab Chip* 6:437–446
- Gracias DH, Tien J, Breen TL, Hsu C, Whitesides GM (2000) Forming electrical networks in three dimensions by self-assembly. *Science* 289:1170–1172
- Graham-Rowe D (2007) Electronic paper rewrites the rulebook for displays. *Nat Photonics* 1:248–251
- Gunther A, Jhunjunwala M, Thalmann M, Schmidt MA, Jensen KF (2005) Micromixing of miscible liquids in segmented gas-liquid flow. *Langmuir* 21:1547–1555
- Hong L, Jiang S, Granick S (2006) Simple method to produce Janus colloidal particles in large quantity. *Langmuir* 22:9495–9499
- Jiang S, Schultz MJ, Chen Q, Moore JS, Granick S (2008) Solvent-free synthesis of Janus colloidal particles. *Langmuir* 24:10073–10077
- Kim SH, Abbaspourrad A, Weitz DA (2011) Amphiphilic crescent-moon-shaped microparticles formed by selective adsorption of colloids. *J Am Chem Soc* 133:5516–5524
- Lan WJ, Li SW, Xu JH, Luo GS (2010) Rapid measurement of fluid viscosity using co-flowing in a co-axial microfluidic device. *Microfluid Nanofluid* 8:687–693
- Lan WJ, Li SW, Xu JH, Luo GS (2011) Controllable preparation of nanoparticle-coated chitosan microspheres in a co-axial microfluidic device. *Lab Chip* 11:652–657
- Li SW, Xu JH, Wang YJ, Lu YC, Luo GS (2009) Low-temperature bonding of poly-(methyl methacrylate) microfluidic devices under an ultrasonic field. *J Micromech Microeng* 19:015035
- Ling XY, Phang IY, Acikgoz C, Yilmaz MD, Hempenius MA, Vancso GJ, Huskens J (2009) Janus particles with controllable patchiness and their chemical functionalization and supramolecular assembly. *Angew Chem Int Ed* 48:7677–7682
- Lu Y, Yin Y, Xia Y (2001) Three-dimensional photonic crystals with non-spherical colloids as building blocks. *Adv Mater* 13:415–420
- Nie ZH, Xu SQ, Seo M, Lewis PC, Kumacheva E (2005) Polymer particles with various shapes and morphologies produced in continuous microfluidic reactors. *J Am Chem Soc* 127:8058–8063
- Nisisako T, Hatsuzawa T (2010) A microfluidic cross-flowing emulsion generator for producing biphasic droplets and anisotropically shaped polymer particles. *Microfluid Nanofluid* 9:427–437
- Nisisako T, Torii T (2007) Formation of biphasic Janus droplets in a microfabricated channel for the synthesis of shape-controlled polymer microparticles. *Adv Mater* 19:1489–1493
- Nisisako T, Torii T, Higuchi T (2002) Droplet formation in a microchannel network. *Lab Chip* 2:24–26
- Paunov VN, Cayre OJ (2004) Supraparticles and “Janus” particles fabricated by replication of particle monolayers at liquid surfaces using a gel trapping technique. *Adv Mater* 16:788–791
- Perro A, Reculosa S, Ravaine S, Bourgeat-Lami EB, Duguet EJ (2005) Design and synthesis of Janus micro- and nanoparticles. *Mater Chem* 15:3745–3760
- Prasad N, Perumal J, Choi CH, Lee CS, Kim DP (2009) Generation of monodisperse inorganic–organic Janus microspheres in a microfluidic device. *Adv Funct Mater* 19:1656–1662
- Saeki D, Sugiura S, Kannamori T, Sato S, Ichikawa S (2010) Microfluidic preparation of water-in-oil-in-water emulsions with an ultra-thin oil phase layer. *Lab Chip* 10:357–362
- Takei H, Shimizu N (1997) Gradient sensitive microscopic probes prepared by gold evaporation and chemisorption on latex spheres. *Langmuir* 13:1865–1868
- Thorsen T, Roberts RW, Arnold F (2001) Dynamic pattern formation in a vesicle-generating microfluidic device. *Phys Rev Lett* 86:4163–4166
- Tung KY, Li CC, Yang JT (2009) Mixing and hydrodynamic analysis of a droplet in a planar serpentine micromixer. *Microfluid Nanofluid* 7:545–557
- Utada AS, Fernandez-Nieves A, Stone HA, Weitz DA (2007) Novel defect structures in nematic liquid crystal shells. *Phys Rev Lett* 99:094502
- Waelchli S, von Rohr PR (2006) Two-phase flow characteristics in gas-liquid microreactors. *Int J Multiph Flow* 32:791–806
- Walther A, Muller AHE (2008) Janus particles. *Soft Matter* 4:663–668
- Wang W, Xie R, Ju XJ, Luo T, Liu L, Weitz DA, Chu LY (2011) Controllable microfluidic production of multicomponent multiple emulsions. *Lab Chip* 11:1587–1592
- Xu JH, Li SW, Tan J, Wan YJ, Luo GS (2006a) Controllable preparation of monodisperse O/W and W/O emulsions in the same microfluidic device. *Langmuir* 22:7943–7946
- Xu JH, Luo GS, Li SW, Chen GG (2006b) Shear force induced monodisperse droplet formation in a microfluidic device by controlling wetting properties. *Lab Chip* 6:131–136